Supporting Information

Carbon dioxide reduction by lanthanide(III) complexes supported by redox-active Schiff base ligands

Nadir jori,[a] Davide Toniolo [a], Bang C. Huynh,[a] Rosario Scopelliti[a] and Marinella Mazzanti*[a]

[a] Institut des Sciences et Ingénierie Chimiques, École Polytechnique Fédérale de Lausanne (EPFL), CH-1015 Lausanne, Switzerland.

*Corresponding authors: E-mail: marinella.mazzanti@epfl.ch, ISIC/EPFL.

Table of Contents

1. NMR spectra

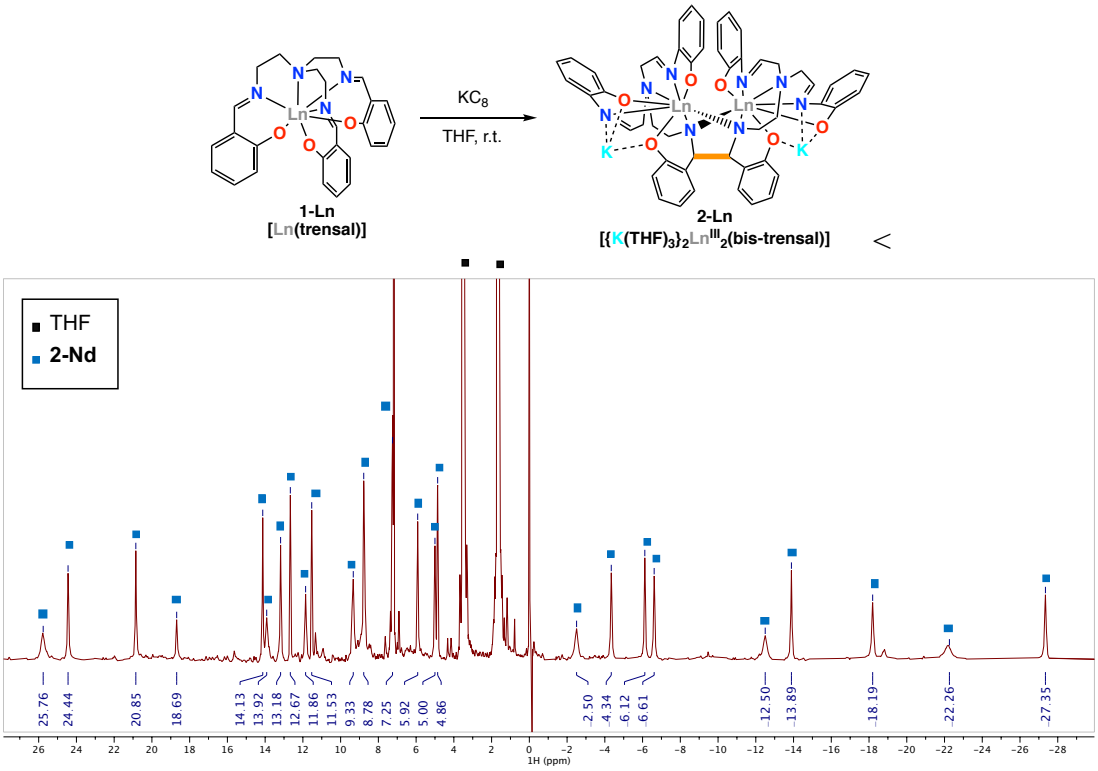

Figure S1: ^{1}H NMR spectrum of **2-Nd** (400 MHz, THF-d$_8$, 298 K).

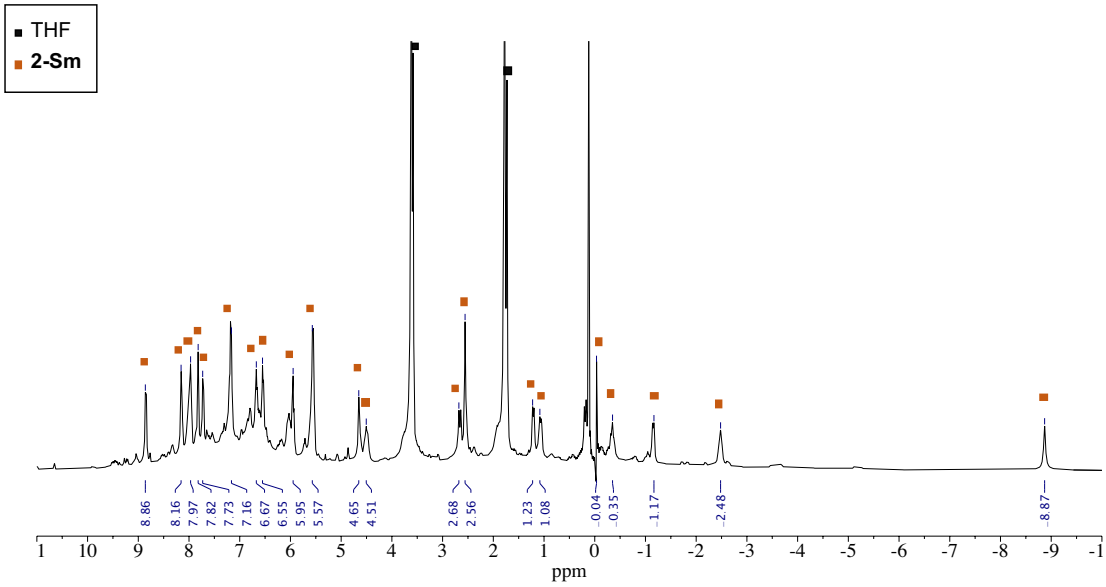

Figure S2: ^{1}H NMR spectrum of **2-Sm** (400 MHz, THF-d$_8$, 298 K).

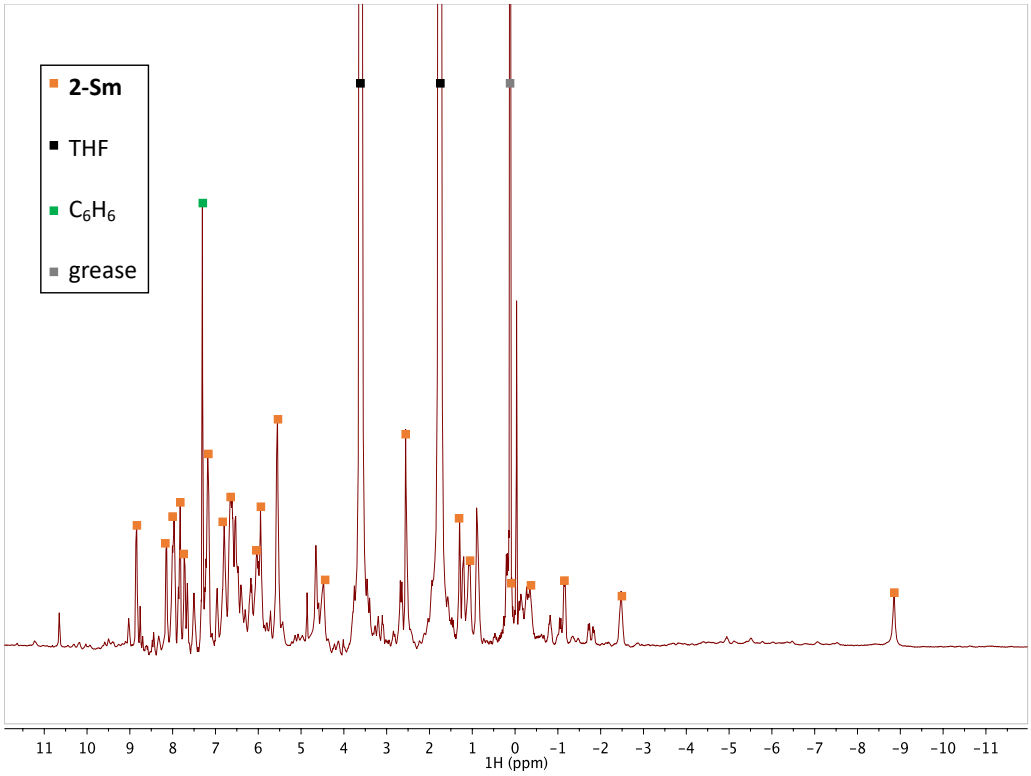

Figure S3: ^{1}H NMR spectrum of the reaction mixture of the synthesis of **2-Sm** starting from [SmI_2] (400 MHz, THF-d_8, 298 K).

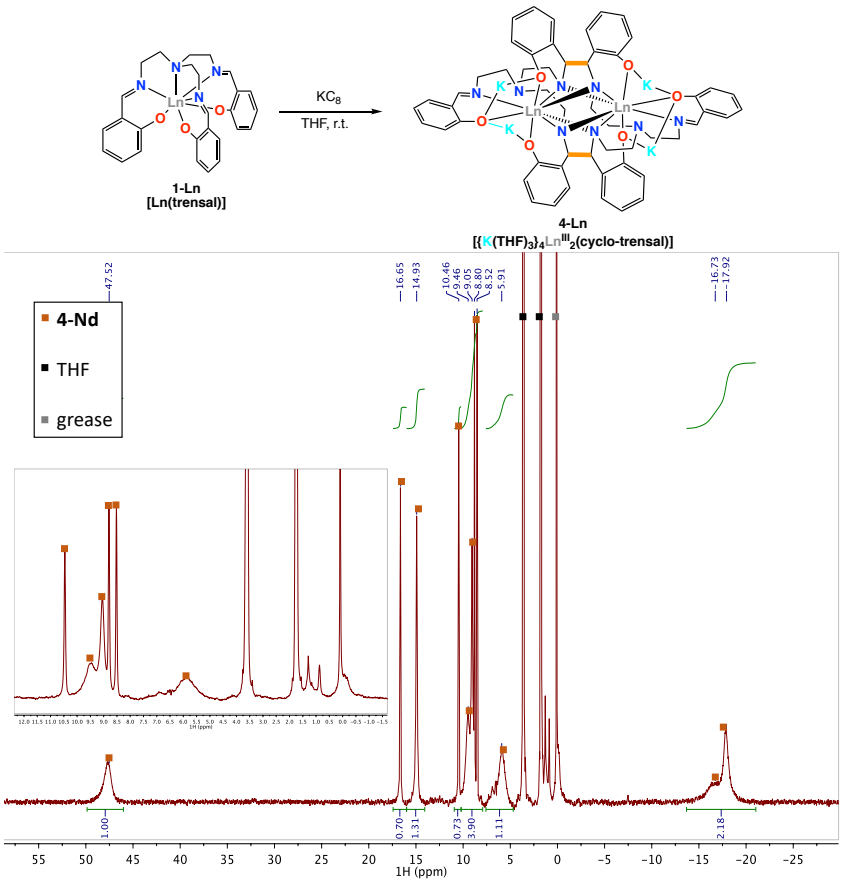

Figure S4: ^{1}H NMR spectrum of **4-Nd** (400 MHz, THF-d_8, 298 K).

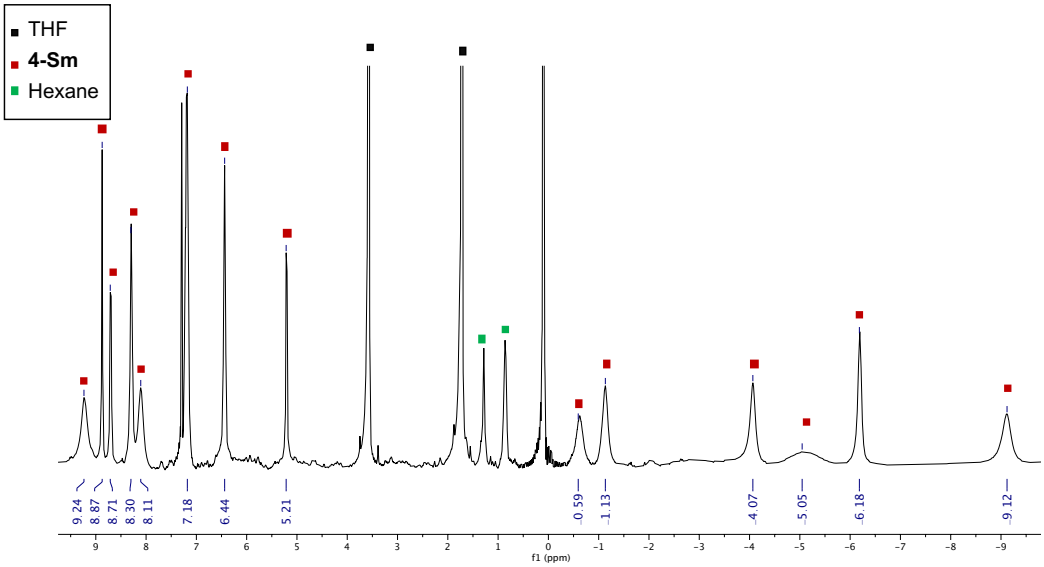

Figure S5: ^{1}H NMR spectrum of **4-Sm** (400 MHz, THF-d_8, 298 K).

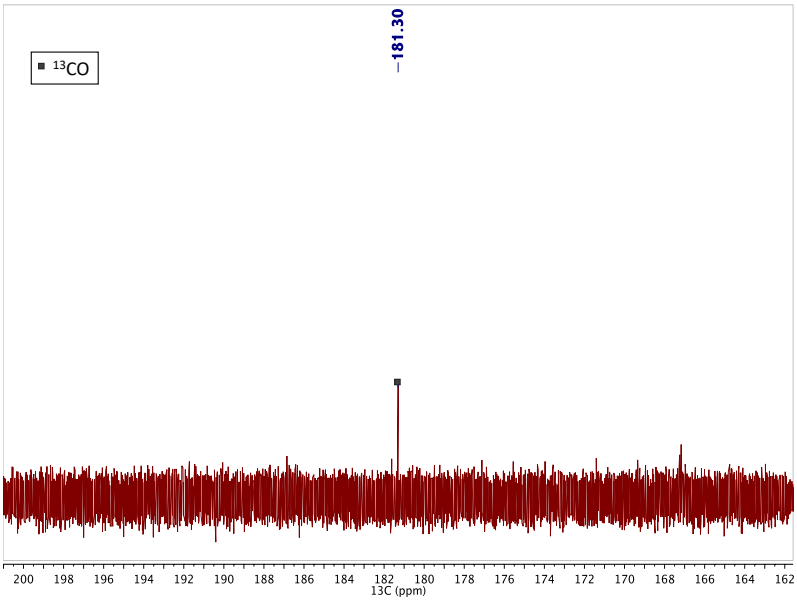

Figure S6: ^{13}C{^{1}H} NMR spectrum of the reaction mixture between **4-Sm** and $^{13}CO_2$ (4 eq) (100 MHz, THF-d_8, 298 K).

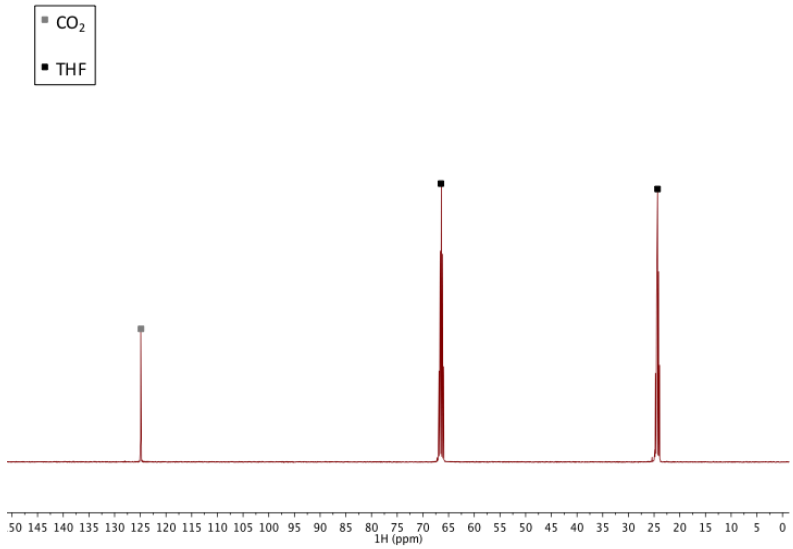

Figure S7: $^{13}C\{^{1}H\}$ NMR spectrum of the reaction mixture between **2-Nd** and $^{13}CO_2$ (2 eq) (100 MHz, THF-d_8, 298 K).

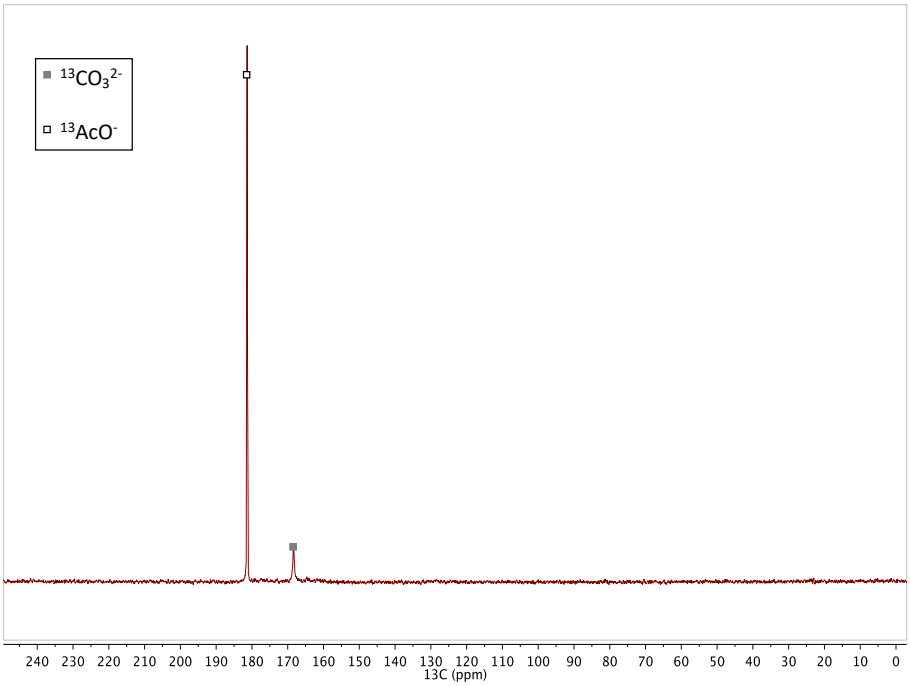

Figure S8 $^{13}C\{^{1}H\}$ NMR spectrum of the residue obtained removing the solvent from the reaction mixture of **2-Nd** and $^{13}CO_2$ (2 eq) after quenching with basic (pD = 13.6) D_2O (D_2O, 100 MHz, 298 K).

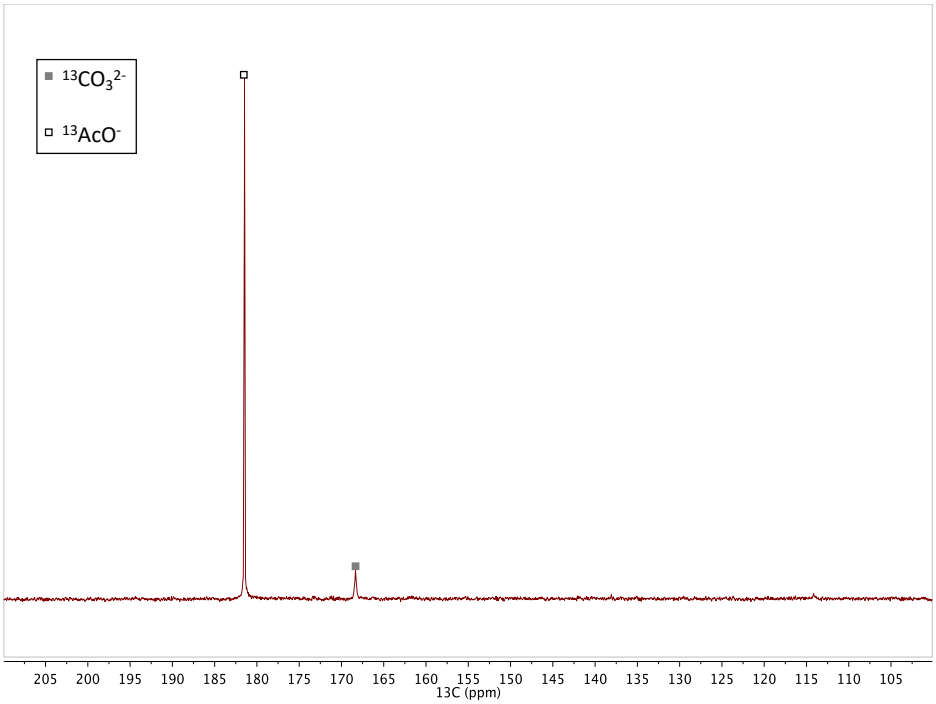

Figure S9 $^{13}C\{^1H\}$ NMR spectrum of the residue obtained removing the solvent from the reaction mixture of **4-Nd** and $^{13}CO_2$ (4 eq) after quenching with basic (pD = 13.6) D_2O (D_2O, 100 MHz, 298 K).

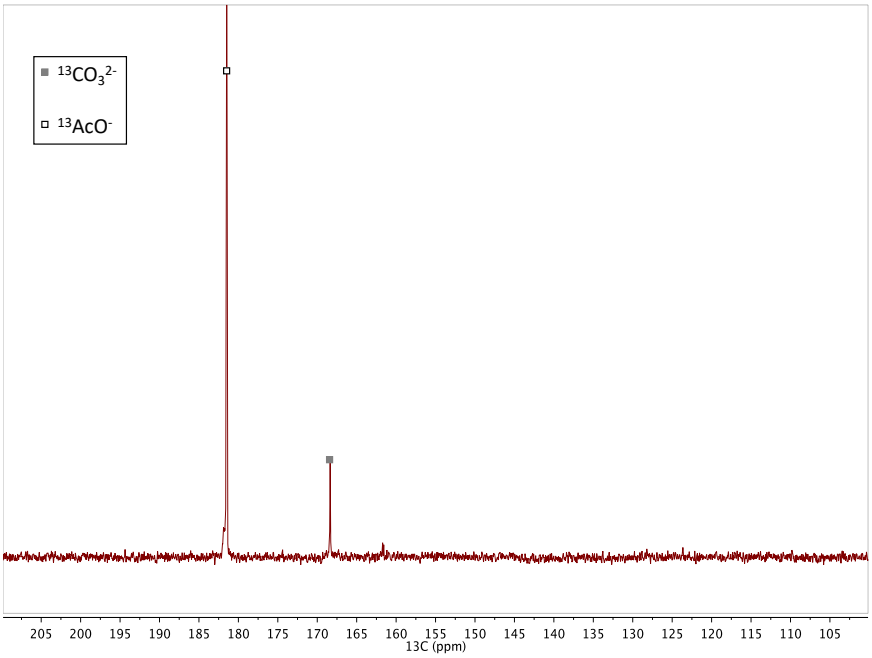

Figure S10 $^{13}C\{^1H\}$ NMR spectrum of the residue obtained removing the solvent from the reaction mixture of **2-Sm** and $^{13}CO_2$ (2 eq) after quenching with basic (pD = 13.6) D_2O (D_2O, 100 MHz, 298 K).

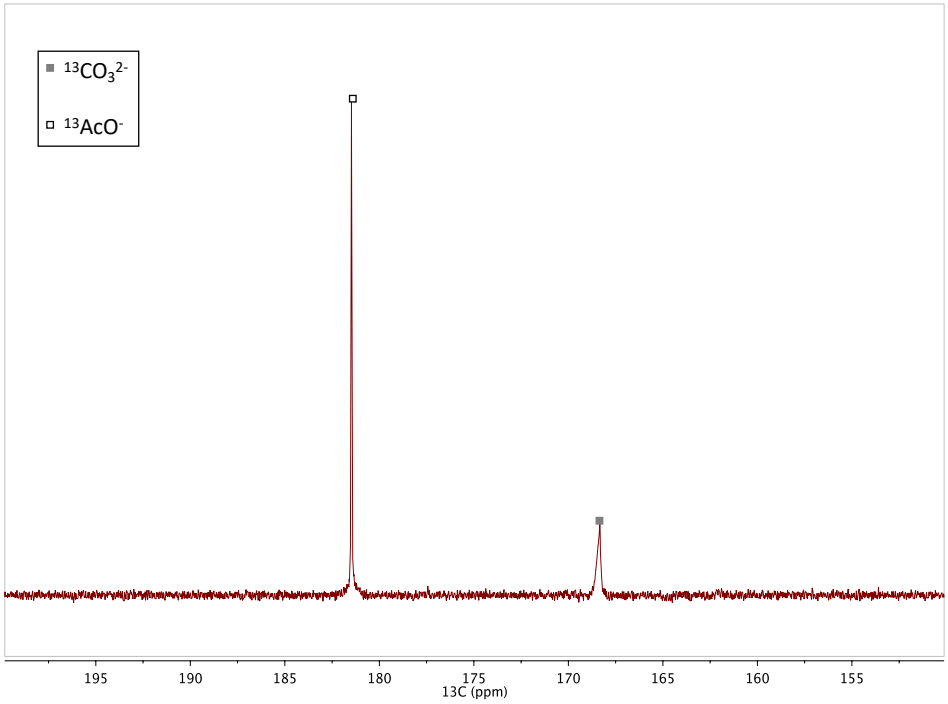

Figure S11 $^{13}C\{^1H\}$ NMR spectrum of the residue obtained removing the solvent from the reaction mixture of **4-Sm** and $^{13}CO_2$ (4 eq) after quenching with basic (pD = 13.6) D_2O (D_2O, 100 MHz, 298 K).

2. X-ray crystallographic data

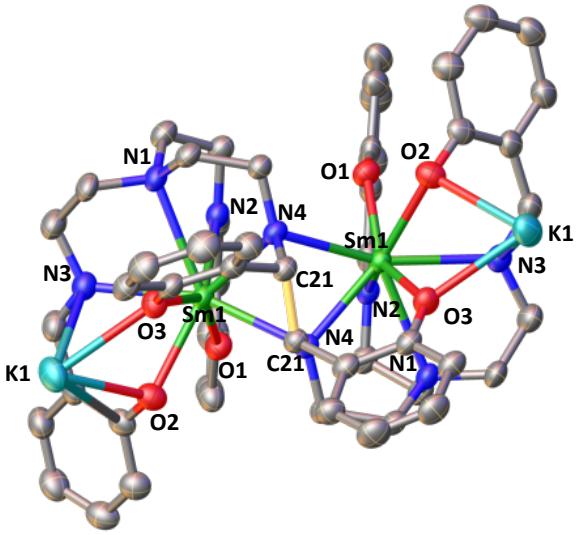

Figure S12 Molecular structure of complex **2-Sm** (C-C bond between imine highlighted in yellow, 50% probability ellipsoid). Hydrogen atoms and THF molecules were omitted for clarity.

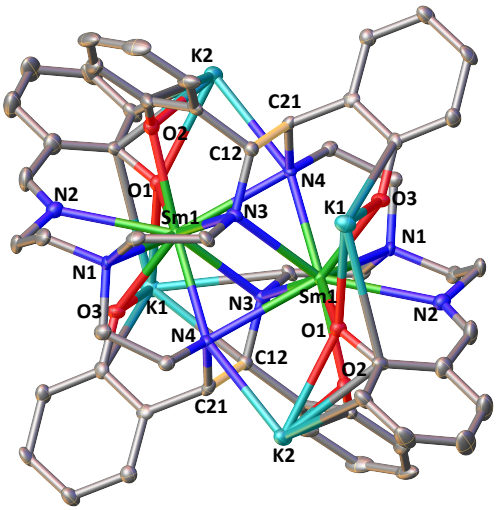

Figure S13 Molecular structure of complex **4-Sm** (C-C bonds between imine highlighted in yellow, 50% probability ellipsoids). Hydrogen atoms and THF molecules were omitted for clarity.

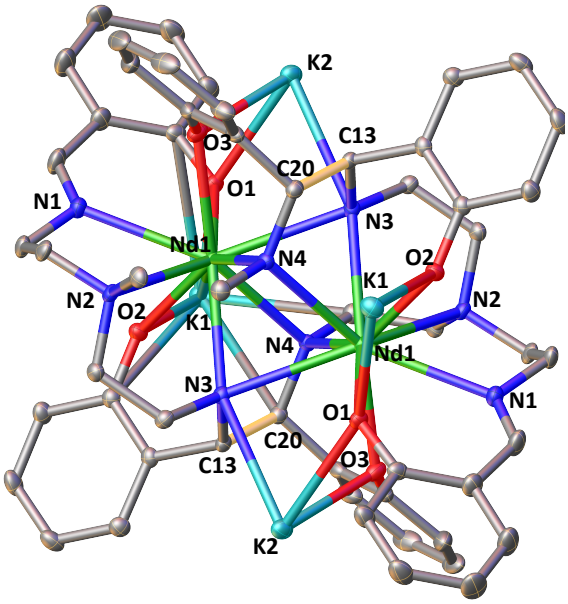

Figure S14 Molecular structure of complex **4-Nd** (C-C bonds between imine highlighted in yellow, 50% probability ellipsoids). Hydrogen atoms and THF molecules were omitted for clarity.

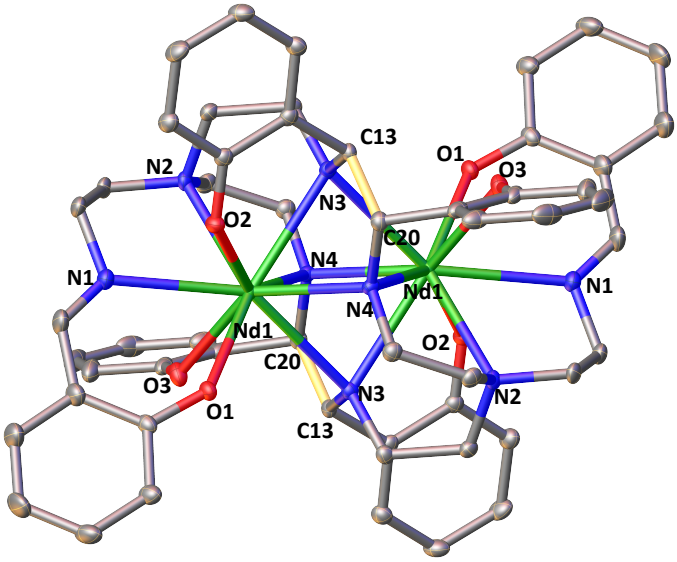

Figure S15 Side view of solid-state molecular structure of complex **4-Nd** (C-C bonds between imine highlighted in yellow, 50% probability ellipsoids). Hydrogen and potassium atoms and THF molecules were omitted for clarity.

Table S1. X-ray crystallographic data.

Compound	**2-Nd**	**2-Sm**	**3-Eu**	**4-Nd**	**4-Sm**
Formula	$C_{78}H_{102}K_2N_8Nd_2O_{12}$	$C_{72.48}H_{90.96}K_2N_8O_{10.62}Sm_2$	$C_{66}H_{78}Eu_2K_2N_8O_9$	$C_{86}H_{118}K_4N_8Nd_2O_{14}$	$C_{86}H_{118}K_4N_8O_{14}Sm_2$
Crystal size [mm]	0.210×0.057×0.047	0.50×0.09×0.06	0.47×0.28×0.25	0.22×0.20×0.14	0.19×0.13×0.12
Crystal system	Monoclinic	Monoclinic	Monoclinic	monoclinic	Monoclinic
Space group	*C* 2/*c*	*C* 2/*c*	*I* 2/*a*	*P* $2_1/n$	*P* $2_1/n$
V [Å^3]	7492.2(6)	7268.8(2)	7096.0(3)	4459.02(15)	4462.4(3)
a [Å]	19.1572(10)	18.9002(3)	16.1474(4)	11.5916(2)	11.5872(5)
b [Å]	19.9660(6)	19.5477(2)	26.3520(7)	17.4426(3)	17.4186(7)
c [Å]	21.4402(9)	21.6120(3)	16.7297(4)	22.1502(4)	22.2099(9)
α [°]	90	90	90	90	90
β [°]	113.990(5)	114.4471(18)	94.589(2)	95.3459(18)	95.457(4)
γ [°]	90	90	90	90	90
Z	4	4	4	2	2
Absorption coefficient [mm^{-1}]	1.549	13.537	14.031	1.403	1.554
F (000)	3520	3315	3064	1996	2004
T [K]	140.00(10)	140.01(10)	140.00(10)	100.01(10)	100.01(10)
Total no. reflexions	53552	25997	7266	70708	55351
Unique reflexions [R_{int}]	12961 [0.0544]	7150 [0.0314]	7266 [0.0380]	11477 [0.0371]	8454 [0.0973]
Final R indice [I>2σ(I)]	0.0400	0.0398	0.0523	0.0258	0.0436
Largest diff. peak and hole [eA^{-3}]	2.049 and -1.467	1.608 and -0.793	1.653 and -0.836	0.760 and -0.904	1.421 and -0.982
GOF	1.038	1.026	1.046	1.043	1.023

3. Electrochemistry

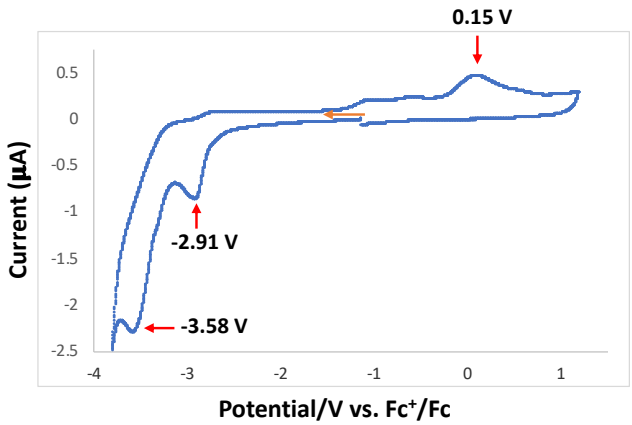

Figure S16 Room temperature cyclic voltammogram of a saturated solution of complex [Nd(trensal)], **1-Nd** recorded in 0.1 M $[NBu_4][PF_6]$ in THF at 100 mV/sec scan rate, referenced against $[Fe(C_5H_5)_2]^+/[Fe(C_5H_5)_2]$.

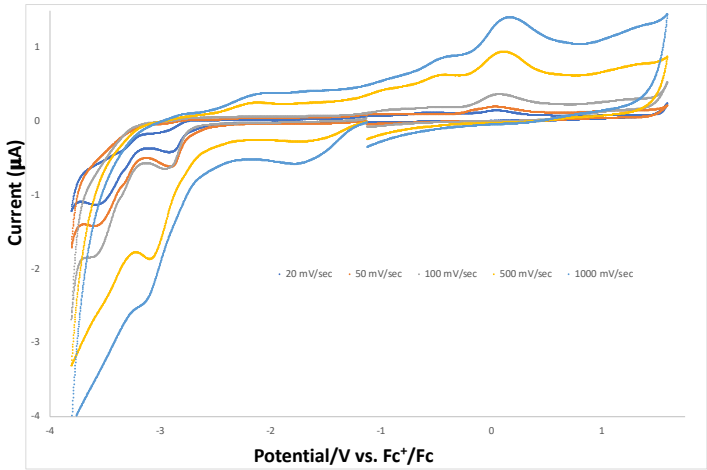

Figure S17 Room temperature cyclic voltammogram of a saturated solution of complex [Nd(trensal)], **1-Nd** recorded in 0.1 M $[NBu_4][PF_6]$ in THF at different scan rates, referenced against $[Fe(C_5H_5)_2]^+/[Fe(C_5H_5)_2]$.

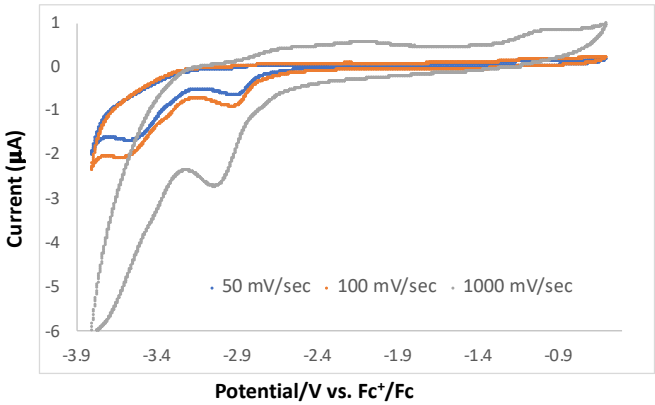

Figure S18 Reduction region of the cyclic voltammogram of a saturated solution of complex [Nd(trensal)], **1-Nd** recorded in 0.1 M $[NBu_4][PF_6]$ in THF at different scan rates, referenced against $[Fe(C_5H_5)_2]^+/[Fe(C_5H_5)_2]$.

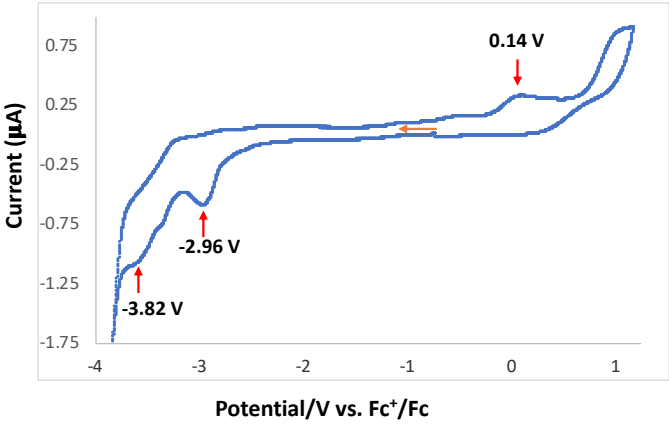

Figure S19 Room temperature cyclic voltammogram of a saturated solution of complex [Sm(trensal)], **1-Sm** recorded in 0.1 M $[NBu_4][PF_6]$ in THF at 100 mV/sec scan rate, referenced against $[Fe(C_5H_5)_2]^+/[Fe(C_5H_5)_2]$.

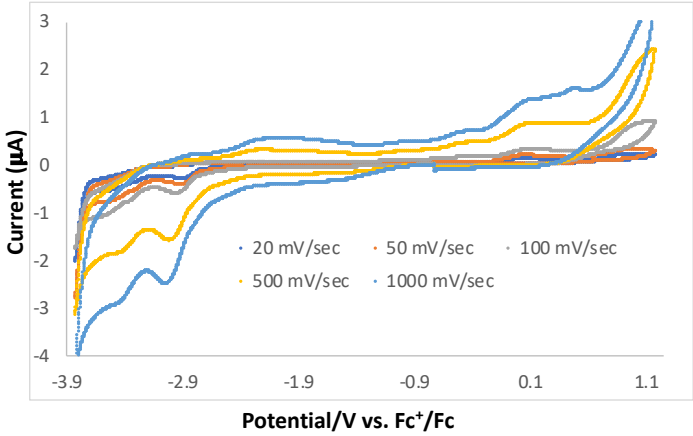

Figure S20 Room temperature cyclic voltammogram of a saturated solution of complex [Sm(trensal)], **1-Sm** recorded in 0.1 M $[NBu_4][PF_6]$ in THF at different scan rates, referenced against $[Fe(C_5H_5)_2]^+/[Fe(C_5H_5)_2]$.

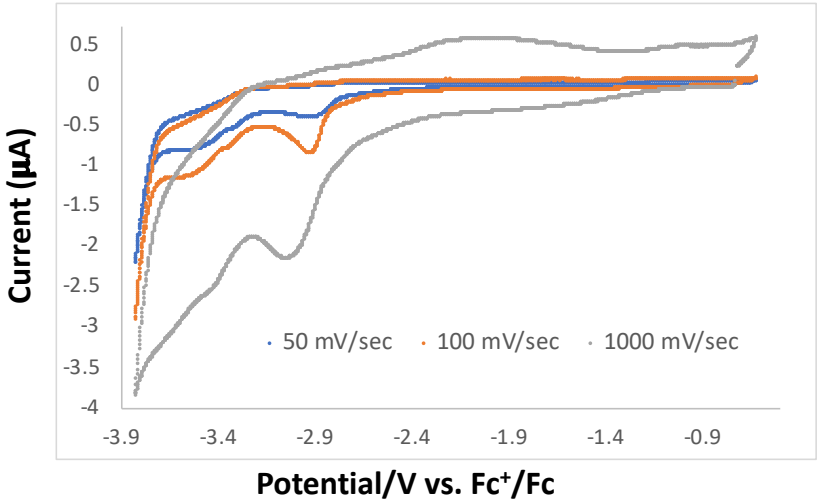

Figure S21 Reduction region of the cyclic voltammogram of a saturated solution of complex [Sm(trensal)], **1-Sm** recorded in 0.1 M $[NBu_4][PF_6]$ in THF at different scan rates, referenced against $[Fe(C_5H_5)_2]^+/[Fe(C_5H_5)_2]$.

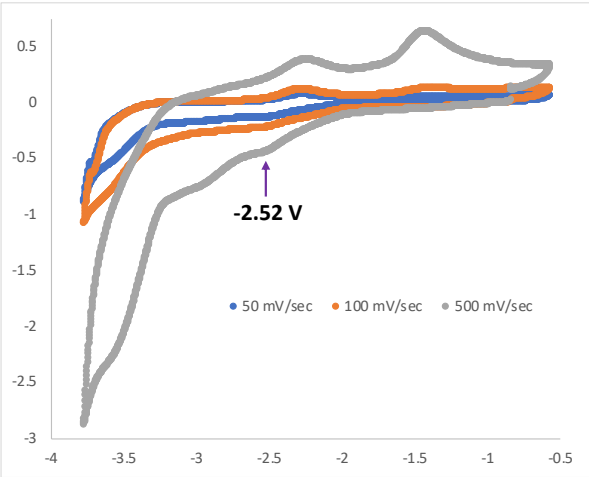

Figure S22 Reduction region of the cyclic voltammogram of a saturated solution of complex [Eu(trensal)], **1-Eu** recorded in 0.1 M $[NBu_4][PF_6]$ in THF at different scan rates (blue: 50 mV/sec, orange: 100 mV/sec and grey: 500 mV/sec) referenced against $[Fe(C_5H_5)_2]^+/[Fe(C_5H_5)_2]$.

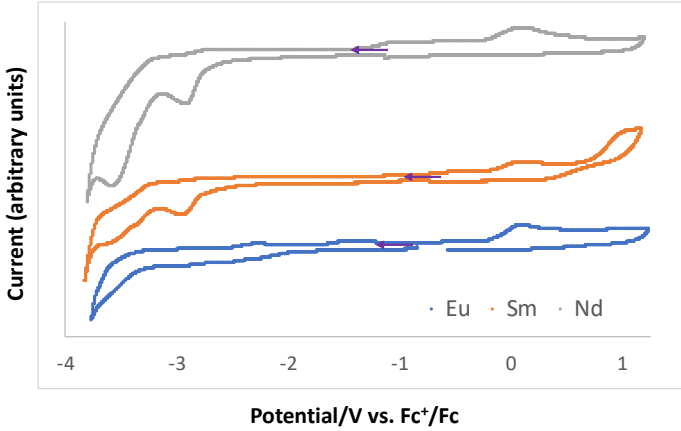

Figure S23 Cyclic voltammograms of complexes **1-Eu** (blue), **1**-Sm (orange) and **1**-Nd (grey) in ~0.1 M $[Bu_4N][PF_6]$ THF solution at 100mV/sec scan rate.